Journal of Molecular Catalysis B: Enzymatic 68 (2011) 139–146

Contents lists available at ScienceDirect

Journal of Molecular Catalysis B: Enzymatic

journal homepage: www.elsevier.com/locate/molcatb

Preparation and characterization of cellulase-bound magnetite nanoparticles

Jason Jordan[a], Challa S.S.R. Kumar[b], Chandra Theegala[a,*]

[a] Louisiana State University, Baton Rouge, LA, United States
[b] Center for Advanced Microstructures and Devices (CAMD), Baton Rouge, LA, United States

ARTICLE INFO

Article history:
Received 14 December 2009
Received in revised form 17 August 2010
Accepted 27 September 2010
Available online 3 November 2010

Keywords:
Cellulase
Cellulose
Immobilization
Magnetite nanoparticles

ABSTRACT

The covalent binding of cellulase enzyme complex to magnetic (Fe_3O_4) nanoparticles via carbodiimide activation was investigated. The size, structure, and morphology of the magnetic nanoparticles were determined using transmission electron microscopy (TEM). The micrographs revealed a mean diameter of 13.3 nm and showed that the magnetic particles remained discrete with no significant change in size after binding of the enzyme complex. Fourier transform infrared (FTIR) spectroscopy and X-ray photoelectron spectroscopy (XPS) indicated binding to the magnetic nanoparticles and suggested a possible binding mechanism. Maximum binding (~90%) occurred at low enzyme loadings (1–2 mg) and the enzyme-to-support saturation point occurred at a weight ratio of 0.02. Thermal measurements for the nanoparticles indicated increased stability over a broader range of temperatures, with a peak relative enzyme activity at 50 °C. The ionic forces between the enzyme and support surface caused a shift in the optimum pH from 4.0 to 5.0.

1. Introduction

Cellulase enzyme complex, composing of endoglucanases, cellobiohydrolyases, and β-glucosidase, is an essential component in the degradation of lignocellulosic residues by various species of fungi, bacteria, and protozoans. Harnessing the hydrolytic prowess of these enzymes allows for efficient conversion of renewable natural resources into fermentable sugars. Unfortunately, the hydrophilic nature of the cellulase complex hinders its practical feasibility when subjected to the complexity of the reactions involved [1].

Immobilization of biomolecules onto insoluble supports is an important tool for the fabrication of a diverse range of functional materials or devices [2]. It provides many distinct advantages including enhanced stability, easy separation from reaction mixture, possible modulation of the catalytic properties, and easier prevention of microbial growth [3]. Of particular interest is the use of magnetic supports for immobilization. Magnetic carrier particles fulfill two functions in that they contain a magnetic material which confers the desired magnetic properties to the ensembles formed with the species to be separated and they can have surface properties which enable a selective separation [4].

In recent years, nano-sized magnetic particles have received increasing attention in various fields, including biomedical and environmental applications, due to their small size, high specific surface area, and low toxicity [5]. More specifically, magnetite (Fe_3O_4) nanoparticles are one of the most prevalent magnetic materials in common use. They are biocompatible super-paramagnetic materials with low toxicity and strong magnetic properties [6], finding applications in intracellular uptake and separation [7–10], drug delivery [11], hyperthermia [9,12], magnetic resonance imaging contrast enhancement [9,13], enzyme and protein immobilization [14–19], and protein purification [20]. Additionally, other fields which benefit from the utilization of magnetic nanoparticles in general and magnetite nanoparticles in particular include waste-water treatment [21,22] and textile processing [23,24].

One of the key factors for utilization of magnetite nanoparticles in biomedical applications is the opportunity to bind biomolecules to their surface. The binding of bioactive substances, such as enzymes, proteins, or antibodies, is commonly accomplished through surface adsorption, covalent bonding, cross-linking with bi-functional reagents, inclusion in a gel phase, or encapsulation [25]. A more recent method involving binding via carbodiimide activation has increased in popularity and is notable due to its simplicity and high efficiency [26].

Immobilization of the cellulase enzyme complex on magnetic supports has also been reported previously [25,27]. However, no studies have been found involving immobilization of the cellulase system on magnetic particles less than 1 μm in size. The purpose of this study was to characterize the cellulase complex

* Corresponding author at: Dept. of Biological & Agricultural Engineering, 149 E.B. Doran Bldg, Louisiana State University, Baton Rouge, LA 70803, United States. Tel.: +1 225 578 1060; fax: +1 225 578 3492.
E-mail addresses: theegala@lsu.edu, ctheegala@agcenter.lsu.edu (C. Theegala).

1381-1177/$ – see front matter © 2010 Elsevier B.V. All rights reserved.
doi:10.1016/j.molcatb.2010.09.010

after direct binding to iron oxide nanoparticles via carbodiimide activation and determine optimum operating conditions. The size and structure of the resultant nanoparticles were characterized by transmission electron microscopy (TEM). The binding of cellulase to magnetite nanoparticles was confirmed using Fourier transform infrared (FTIR) spectroscopy and X-ray photoelectron spectroscopy (XPS). Operating parameters for immobilized cellulase were evaluated using varying pH and thermal conditions, in addition to the binding efficiency of enzyme to support, for determination of conditions which would allow for optimum hydrolysis reactions.

Immobilization of enzymes can have a wide variety of applications. Of particular interest for this and future research is to develop a method for reducing the overall costs which the expensive cellulase enzymes contribute to the ethanol production industry. Cellulase-bound particles could potentially be recovered and recycled to further extend their use for processing of cellulosic materials.

2. Materials and methods

2.1. Materials

Cellulase enzyme complex preparation was provided by Genencor (Rochester, NY). Ammonium hydroxide, Rochelle salts (Na-K tartrate), Na-metabisulfite, citric acid monohydrate, and D-glucose were purchased from Fisher (Fair Lawn, NJ). Ferrous chloride tetrahydrate and ferric chloride were the products of Fluka (Buchs) and Sigma (St. Louis, MO), respectively. 3,5-Dinitrosalicylic acid and microcrystalline cellulose substrate were the guaranteed reagents of Sigma. Sodium hydroxide and 1-(3-dimethylaminopropyl)-3-ethylcarbodiimide hydrochloride (EDC) were supplied by E. M. Science (Cherry Hill, NJ) and Merck (Germany), respectively. Bio-Rad reagent for protein assay was obtained from Bio-Rad Laboratories (Hercules, CA). The water used throughout this study was de-ionized and filtered using a U.S. Filter purification system.

2.2. Preparation of magnetite nanoparticles

Magnetite nanoparticles (Fe_3O_4) were prepared by co-precipitating Fe^{2+} and Fe^{3+} ions by ammonia solution and treating under hydrothermal conditions [14,28]. A 2:1 molar ratio of ferric and ferrous chlorides was dissolved in water under inert conditions. Chemical precipitation was achieved at 25 °C under vigorous stirring by adding 28% NH_4OH solution. The precipitates were heated to 80 °C for 30 min, and then washed three times with water and one time with anhydrous ethanol. The particles were then dried by purging with nitrogen for 24 h and recovered.

2.3. Cellulase immobilization

For binding of the cellulase enzyme, 50 mg of magnetic nanoparticles were added to a 5 ml solution containing 8 mg/ml carbodiimide (EDC). The mixture was then sonicated for 3 min and refrigerated for 30 min until the temperature reached 4 °C. 1 ml of enzyme solution (0–25 mg/ml in water) was then added and followed with sonication for an additional 3 min. The reaction mixture was stored at 4 °C and sonicated at 1 h intervals to ensure uniform dispersion. After 2 h, the mixture was sonicated a final time and heated to 25 °C. The cellulase-bound nanoparticles were recovered by placing the container on a strong permanent magnet. They were washed two times in water and the resultant supernatants were used for protein analysis. The remaining precipitates were then analyzed for enzymatic activity and stability.

2.4. Characterization

The size and morphology of iron oxide nanoparticles before and after enzyme immobilization were determined by TEM using a JEOL 100-CX electron microscope. The binding of cellulase to the nanoparticle surface was determined using the Bradford protein assay. The protein found in the removed supernatant was measured by a colorimetric method involving the binding of Coomassie Brilliant Blue G-250 to the protein and then measuring the concentration across a wavelength of 595 nm [29]. Bio-Rad dye reagent was used for the protein assay and bovine serum albumin as the standard. The binding of the enzyme was confirmed by Fourier transform infrared spectroscopy using a Thermo Nicloet Nexus 670 FTIR model and by X-ray photoelectron spectroscopy (XPS) using a Kratos Axis 165 XPS/Auger.

3,5-Dinitrosalicylic acid (DNS) is an aromatic compound which reacts with reducing sugars and other reducing compounds to form 3-amino-5-nitrosalicylic acid, which absorbs light strongly at 540 nm [30]. The DNS method was used in this study to determine the amount of glucose formed as reducing sugars resulting from a reaction with dinitrosalicylic acid reagent. Sugars that are contained in polysaccharides, such as cellulose and starch, or other complex organic compounds, are not accounted for by this method. D-Glucose was used as the standard.

2.5. Activity measurements

The enzymatic activity was determined by measuring glucose production after a reaction of nanoparticle-bound cellulase with microcrystalline cellulosic substrate [31]. After initial binding, 0.5 ml of solution containing the enzyme-bound particles was added to 50 mg of cellulosic substrate and 1 ml of buffer (0.05 M citrate buffer, pH 5.0). The resulting mixture was allowed to incubate at 50 °C for 1 h, after which 3 ml of DNS reagent was added to stop the reaction [32]. The samples were heated in a boiling water bath for 5 min to allow color formation. They were then cooled and centrifuged for an additional 5 min. The reducing sugar concentration in the resulting supernatant was then measured at 540 nm on a Genesys 20 single beam spectrophotometer. In order to compensate for any interference, a series of blanks were measured in the same manner, one containing enzyme alone and another containing substrate alone. Any absorbance responses measured by the spectrophotometer from these blanks were subtracted from the primary hydrolysis reaction to obtain an accurate measurement. For the purposes of this study, enzymatic activity was measured as the amount of glucose produced (in μmol) per milligram of enzyme used over time, and is stated as IU/mg.

Unless otherwise stated, the activity of free enzyme was measured following similar procedures and conditions as stated for the bound cellulase. In addition, all samples performed in this study were measured in triplicate to obtain an average and promote accuracy. It should be noted, however, that few samples contained outliers which amplified the resulting standard error. These outliers were omitted, resulting in duplicate measurements, in order to minimize error deviations. Contamination is one possible explanation for the reduced quality of the mentioned samples as the sterility of the laboratory environment was not ideal. At the time of this study, the said lab was also being used as a teaching laboratory and was known to contain additional airborne microorganisms. That being said, however, all proper sanitary precautions were taken to produce the most accurate data possible throughout this study and the overall results are believed to reflect this.

2.6. Optimization

The binding efficiency of enzyme to magnetic particles was determined by first evaluating the saturation of cellulase enzyme on the surface of the precipitates. Subsequently, the ideal weight ratio (weight enzyme:weight of nanoparticles) was then determined in order to find the optimum condition allowing for maximum activity. Weight ratio was determined by measuring the mass of immobilized enzyme as indicated by Bradford [29] and associating this value with the mass of corresponding nanoparticles. The mass of Fe_3O_4 nanoparticles was kept constant at 50 mg.

The effect of pH on activity was evaluated using buffers of various pH values. For pH 3, 0.1 M potassium phthalate buffer was used. For pH 4, 0.1 M sodium acetate buffer was used. For pH 5, citrate buffer was used. For pH 6, potassium phosphate buffer was used; and sodium phosphate buffers were used for pH 7 and 8. Hydrolysis reactions were performed using 8.57 mg of cellulase-bound nanoparticles, 50 mg of microcrystalline cellulose, and 1 ml buffer.

For the optimum temperature study, various temperatures were examined spanning a range from 25 °C to 80 °C and the corresponding activity was measured for each. Similar reactor conditions were implemented for this study as were demonstrated with the pH optimization, except that 1 ml of 0.1 M citrate buffer (pH 5.0) was used for all hydrolysis reactions. The pH 5.0 was decided based on results from pH optimization experiments. For both temperature and pH studies, an equal amount of free cellulase enzyme (0.23 mg), as was immobilized on the Fe_3O_4 nanoparticles, was tested for activity comparisons.

2.7. Reusability assay

Cellulase enzyme complex (4.3 mg) immobilized on 120 mg of Fe_3O_4 nanoparticles were subjected to a hydrolysis reaction with microcrystalline cellulose for 96 h. After the specified reaction time, the enzyme-bound nanoparticles were magnetically separated and introduced into solution containing fresh substrate. Activity was determined following each 96 h recycle until the activity had fallen below 10%.

Additionally, a series of controls were measured in order to compensate for any interference, one containing enzyme alone and another containing substrate alone. Any responses measured by the spectrophotometer from these controls were subtracted from the primary hydrolysis reaction to aide in increasing accuracy among measurements. All samples were measured in triplicate.

3. Results and discussion

3.1. Nanoparticle size and morphology

The TEM images of magnetic nanoparticles without (a) and with (b) immobilized cellulase enzymes are shown in Fig. 1 along with their corresponding size distributions. Unbound Fe_3O_4 par-

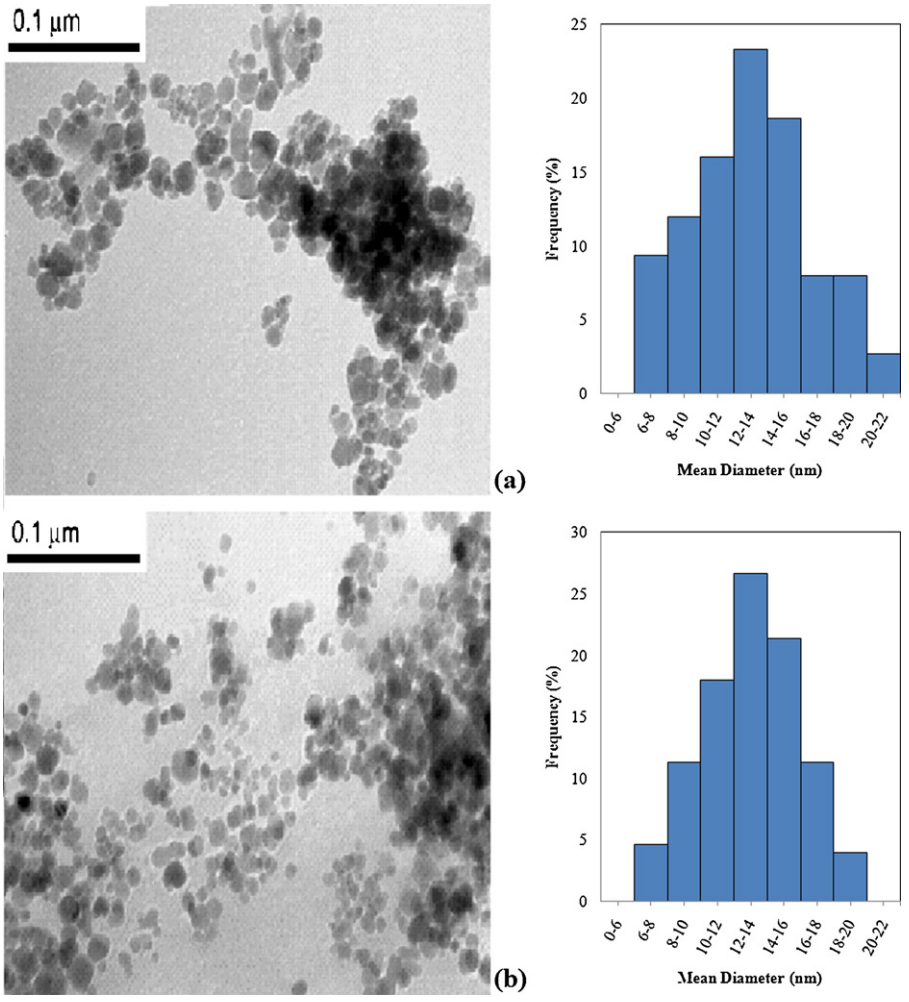

Fig. 1. Transmission electron microscopy (TEM) images of magnetic nanoparticles without (a) and with (b) immobilized cellulase. Weight ratio (enzyme solution/Fe_3O_4) = 0.028 (w/w).

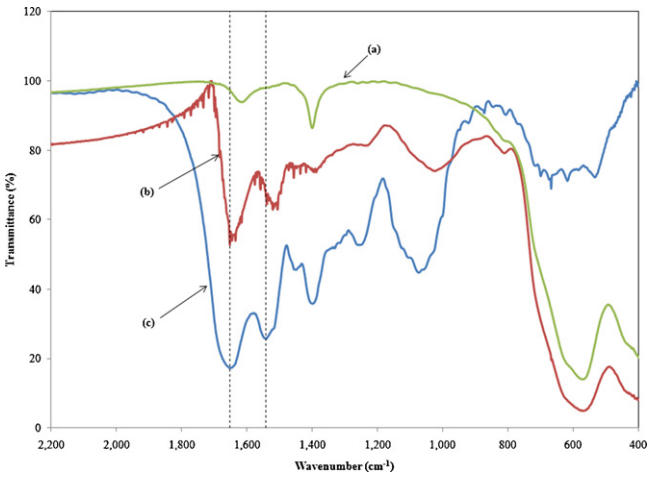

Fig. 2. FTIR spectra of magnetite nanoparticles without (a) and with (b) bound cellulase, and free cellulase enzyme complex (c).

ticles appear to be somewhat polydisperse ranging from 6 to 20 nm in diameter, respectively. The particles have an overall mean diameter of 13.28 ± 3.9 nm. After binding of the cellulase enzyme, the nanoparticles remained discrete and had a mean diameter of 13.31 ± 3.2 nm. A total of 150 particles were randomly chosen from both images for statistical analysis to determine if there was any significant difference in size between the bare iron oxide nanoparticles and the nanoparticles containing the bound cellulase enzyme complex. A 95% confidence interval was constructed indicating that the difference between the two population means was most likely in the range (−0.402, 0.432). Statistical analysis suggests that the binding process did not cause any significant change in size ($\alpha = 0.05$, p-value = 0.976); and, from physical inspection of the images, it is noticeable that no additional aggregation occurred as a result.

3.2. Mechanism for enzyme immobilization

The binding of the cellulase enzyme complex to magnetite nanoparticles was confirmed by FTIR and XPS. Fig. 2 shows the FTIR spectra for the naked Fe_3O_4 nanoparticles, enzyme-bound Fe_3O_4, and the solid state crude enzyme preparation. The characteristic IR frequencies at 1653 and 1542 cm^{-1} on the cellulase enzyme complex are also present on the nanoparticles containing immobilized cellulase, therefore suggesting attachment of the enzyme to Fe_3O_4 nanoparticles. These particular frequencies most likely represent the stretching of C=O and C–O groups. A shift in frequency from 1542 cm^{-1} to 1522 cm^{-1} on the immobilized enzyme is likely due to the formation of an amide bond (Fig. 3) resulting from the reaction between a carboxyl group on the enzyme and an amine group on the nanoparticle surface (specifically, the C–O to C–N conversion). The naked Fe_3O_4 nanoparticles also show a characteristic frequency at 1618 cm^{-1} which may be due to N–H stretching of the amine functional group. This peak is no longer present with the immobilized cellulase enzyme, further indicating an amide bond formation. The weaker bands for the immobilized cellulase are essentially a result of low enzyme loading on the nanoparticle surface.

Fig. 4 displays an XPS spectrum for samples containing pure Fe_3O_4 nanoparticles and Fe_3O_4 nanoparticles with the cellulase complex attached. Characteristic peaks at 398.6 and 284.6 eV on the enzyme-bound nanoparticles indicate a heavy loading of nitrogen and carbon which are not present on the unbound nanoparticles. These peaks suggest attachment of the enzyme complex as this increase in nitrogen and carbon can be attributed to the amine and carboxyl groups found on the cellulase enzyme.

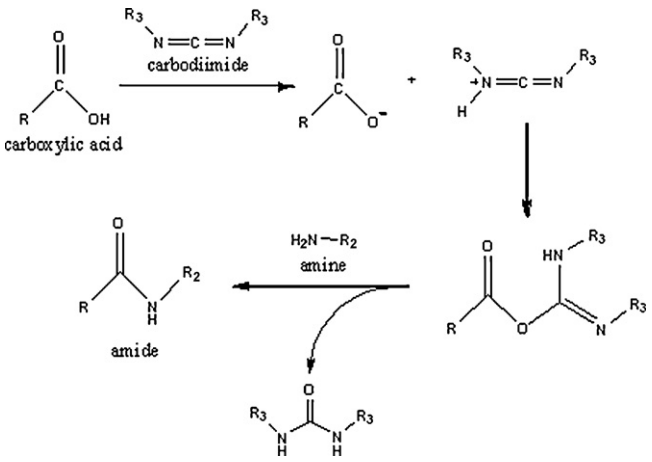

Fig. 3. Synthesis involving amide bond formation via carbodiimide activation.

Of particular interest are the concentrations of the individual elements which are shown in Table 1. An atomic concentration of 39.51% for carbon on the enzyme-bound nanoparticles results in a 33.27% increase from the unbound nanoparticles. The atomic concentration of nitrogen increased to 8.13% on the enzyme-bound nanoparticles, whereas there was none detected on the unbound nanoparticles.

3.3. Binding efficiency

By assaying the amount of protein found in the supernatant after the enzyme binding process, it was determined that when the amount of Fe_3O_4 nanoparticles was kept constant at 50 mg, the results displayed a higher level of bound enzyme (measured as protein) when low enzyme loadings were administered. The

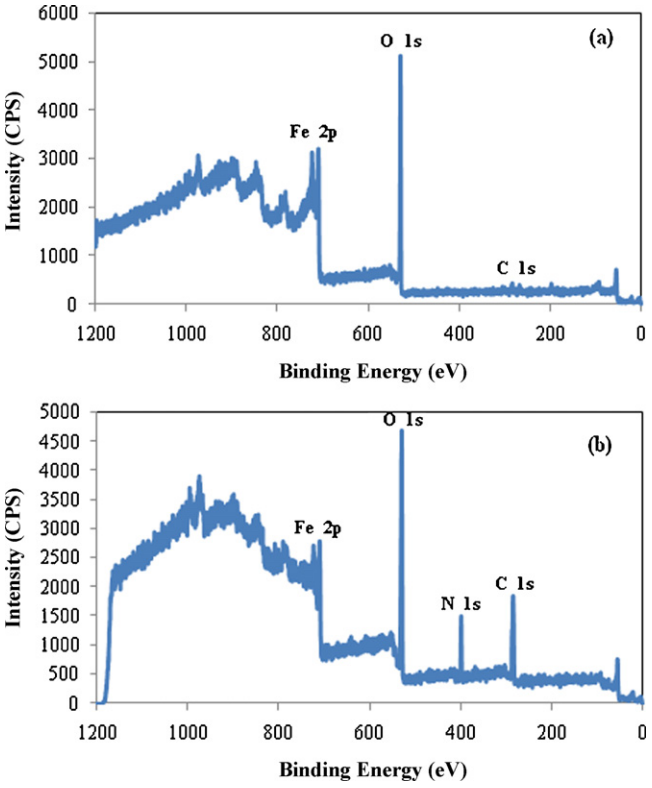

Fig. 4. XPS analysis of pure Fe_3O_4 nanoparticles (a) and cellulase-bound Fe_3O_4 nanoparticles (b).

Table 1
Elemental analysis of pure and enzyme-bound Fe_3O_4 from evaluation by XPS.

	Peak	Position BE (eV)	FWHM (eV)	Raw area (CPS)	RSF	Atomic mass	Atomic concentration (%)	Mass concentration (%)
Pure Fe_3O_4	Fe 2p	709.1	4.570	36688	2.957	55.85	54.74	81.38
	C 1s	283.6	1.638	466.5	0.278	12.01	6.240	2.000
	N 1s	nd[a]	nd	nd	nd	nd	nd	nd
	O 1s	528.7	1.376	7554	0.780	16.00	39.02	16.62
Enzyme-bound Fe_3O_4	Fe 2p	709.8	4.607	29652	2.957	55.85	22.74	54.46
	C 1s	284.6	3.259	5742	0.278	12.01	39.51	20.34
	N 1s	398.6	1.815	1962	0.477	14.01	8.130	4.880
	O 1s	529.1	2.711	11156	0.780	16.00	29.61	20.31

[a] nd: none detected.

most efficient level of enzyme binding occurred when 1 mg of free enzyme complex was added at the initiation of the reaction. At this level, more than 90% had become immobilized. It was determined that a limit existed for the amount of enzyme that could bind to the nanoparticle surface as the percentage of bound enzyme decreased exponentially as the amount of enzyme added was increased from 1 mg to 18 mg. Fig. 5 depicts the saturation point for enzyme binding. A number of reasons could be contributed to the saturation limit in binding, but some of the most plausible explanations include surface area saturation and limited availability of binding sites. To confirm the level of enzyme binding the resulting analysis of the Bradford assay is displayed in Table 2, indicating the mass of measured protein found in the removed supernatant following the binding process along with two additional washings of the final product. An apparent level of error is associated with the analysis which is evident from the mass of protein found at the initial zero concentration. This error would also be associated with the initial mass of protein for each subsequent concentration added to the solution as the same protein analysis was performed to signify the amount of enzyme present; therefore, no correction factor was assessed. It is evident that the majority of enzyme was lost during extraction of the original supernatant (denoted as S1), however, trace amounts are also present in the wash (S2 and S3) which become more distinct as the amount of initially added enzyme increases.

Table 2
Unbound protein found in multiple supernatant washes determined via protein assay. The remainder of the protein added was considered bound to the Fe_3O_4 nanoparticles.

Protein added (mg/ml)	Supernatant removed	Protein in wash (mg)
0	S1	0.211
	S2	0.343
	S3	0.142
1	S1	0.193
	S2	0.008
	S3	0.002
3	S1	1.908
	S2	0.033
	S3	0.007
6	S1	4.475
	S2	0.113
	S3	0.023
12	S1	9.791
	S2	0.229
	S3	0.019
18	S1	14.708
	S2	0.490
	S3	0.081

3.4. Optimization for enzyme binding

By assaying the amount of unbound enzymes (measured as protein) in the supernatant after immobilization and measuring their corresponding activity, the optimum weight ratio of bound enzyme to nanoparticles was determined. An initial loading of 50 mg of magnetic Fe_3O_4 was kept constant for this process and enzyme loading was increased, as was carried out with the determination of binding efficiency. The maximum weight ratio achieved was determined to be 0.16.

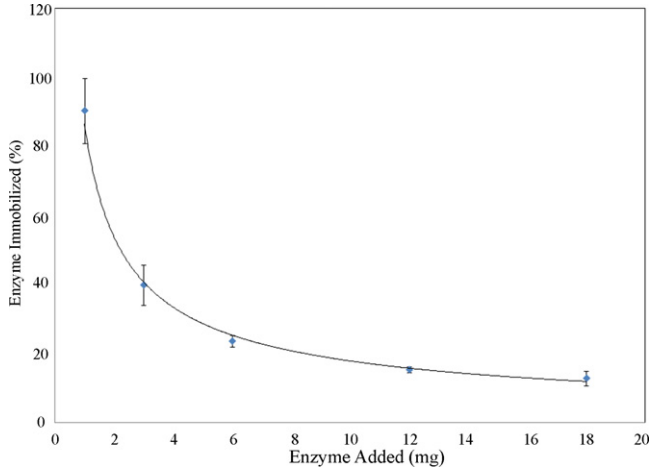

Fig. 5. Binding efficiency for varying amounts of protein added to 50 mg of Fe_3O_4 nanoparticles.

It has been proposed that enzyme which is too heavily saturated upon the surface of the nanoparticles will, in effect, cause a steric hindrance between enzyme molecules by blocking active binding sites from reaching the substrate and, therefore, causing an overall reduction in activity. As shown in Table 3, the point of saturation for the enzyme complex on the nanoparticle surface appears to be 0.02

Table 3
Activity values for varying ratios of bound cellulase enzyme to Fe_3O_4 nanoparticles.

Cellulase added (mg)	Cellulase bound (mg)	Weight ratio (mg bound enzyme/mg nanoparticles)	Activity (IU/mg)	Relative activity (%)
0	0	0	0	0
1	0.782	0.016	40.14	63.97
3	1.042	0.021	62.75	100
6	1.409	0.028	33.07	52.70
18	2.722	0.054	25.42	40.51
21	4.181	0.084	22.96	36.59
25	7.973	0.159	12.16	19.37

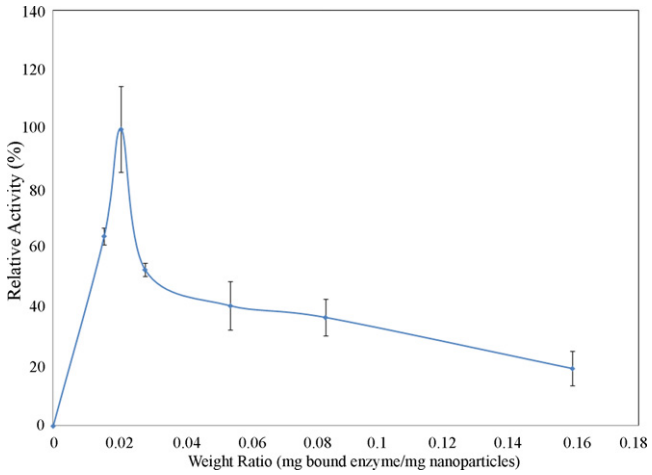

Fig. 6. Relative activity values corresponding to immobilized enzyme weight ratios.

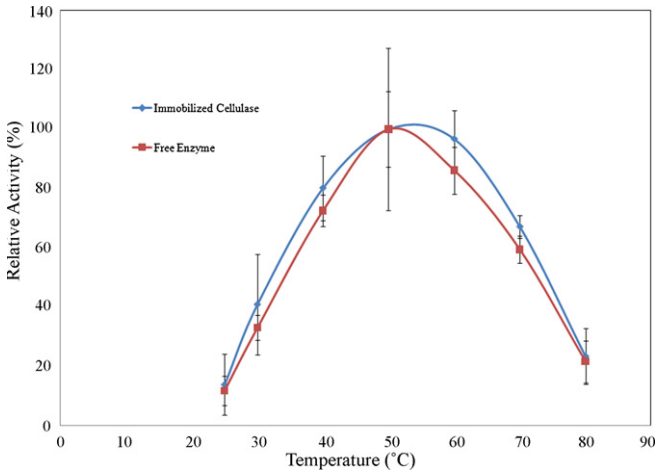

Fig. 8. Effect of temperature on activity of free and immobilized cellulase at pH 5.0.

as it attained a maximum activity value of 62.7 IU/mg. The relative activity curve for the varying weight ratios is shown in Fig. 6.

The pH dependency of an enzyme is dependent on the nature of its functional groups. The total charge on an enzyme's active sites determines if the enzymes optimum operability will result from an acidic or basic microenvironment. However, coupling of an enzyme to a support, whether charged or uncharged, will typically cause a shift in the ideal pH. Generally, the greater the charge on the support, the greater the effect, particularly if the substrate is charged as well [33,34]. The binding protocol for this experiment used positively charged amino groups for immobilization, therefore an alteration in the ionic atmosphere and total shift in the optimum pH was expected. As shown in Fig. 7, the maximum activity for immobilized cellulase complex occurred under a pH of 5.0, which indicates an increase in net negative charge of the immobilized enzyme as compared to an optimum pH of 4.0 for the free enzyme. The pH of the environment becomes lower than that of the bulk solution as a result.

Immobilization of an enzyme can cause changes in its thermal characteristics which will generally incite an apparent improvement in stability. However, an increase in temperature can also increase protein denaturation, which can occur as a result of changes in tertiary structure, oxidation of some labile groups, or some other physical modification of the protein [35]. In effect, activity is reduced along an exponential decay. The immobilized cellulase complex demonstrated an optimum activity at a temperature of 50 °C.

Disruption of weak intramolecular forces and subsequent unfolding of the protein chain in free enzymes can be caused by thermal deactivation [25]. Immobilization of the cellulase complex can increase the thermal stability by stabilizing the weak ionic forces and hydrogen bonds and thus increasing the range of operating temperatures. This was also depicted in the present study and is shown in Fig. 8. However, only a marginal increase was displayed over that of the free enzyme and the differences are not likely to be of statistical significance.

Typically, the resulting level of activity is reduced when enzymes are immobilized via covalent bonding. This is likely due to bonding of key functional groups positioned within the active site and thus preventing substrate interactions [36]. This was also observed in the present study; however, a slight increase in stability was achieved as a result of the immobilization process. The difference in relative activity produced from both free and immobilized enzyme was minimal, however; and therefore, would not prove to be highly beneficial for our purposes.

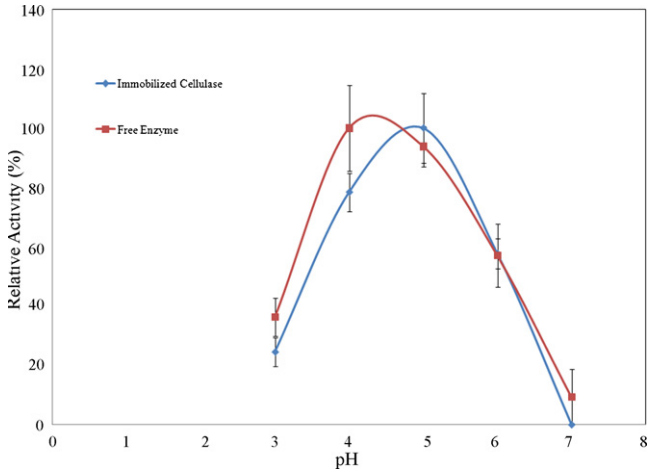

Fig. 7. Effect of pH on activity of free and immobilized cellulase at 50 °C.

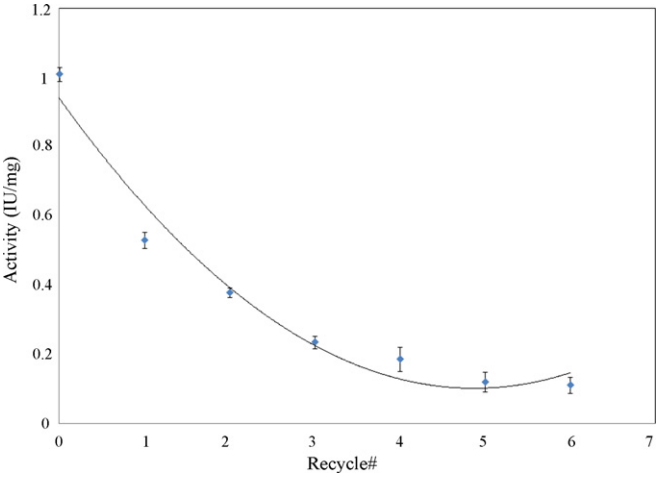

Fig. 9. Activity loss over 6 recycles of cellulase enzyme complex immobilized on Fe_3O_4 nanoparticles.

3.5. Reusability

For practical applications, the reusability of immobilized cellulase enzymes is considered to be of high importance. As a result of this study, the immobilized cellulase complex was recycled a total of six times before the residual activity had fallen to approximately 10%. The corresponding activity measurements were determined following each recycle and the overall trend is presented in Fig. 9. The activity of immobilized enzyme was determined to be 30.2% of the free enzyme activity following the initial hydrolysis reaction.

An apparent loss in activity was observed following each recycle with the majority (47.5%) being lost following the initial reaction. This resultant loss in activity could have been attributed to a multitude of factors, which may have included protein denaturation, end-product inhibition, and/or loss of one or more individual components of the cellulase complex. Another possible reason could be modification of the enzymes structure due to carbodiimide activation. The individual enzymes composing the cellulase complex each contain a large number of functional groups available for immobilization, many of which are located on the active site of the enzyme and are specific to cleaving the individual linkages between glucose monomers of the cellulosic substrate. Should one of the functional groups located on the active site of the enzyme be involved in immobilization, a large decrease in stability of the enzyme could result.

4. Conclusions

A crude cellulase enzyme complex was successfully immobilized on magnetic Fe_3O_4 nanoparticles via carbodiimide activation and characterized. The pure Fe_3O_4 particles were analyzed using TEM and were determined to have an average diameter of 13.28 nm. Enzyme-bound particles showed no significant change in size and it was determined that no additional agglomeration occurred due to the binding process. Enzyme attachment was confirmed using FTIR and XPS. Enzymatic activity was determined by measuring glucose as reducing sugars using the DNS method. Saturation of the cellulase enzymes on a magnetic support is useful for determining maximum binding ability without further hindering enzymatic activity. Maximum efficiency for enzyme-to-support binding was verified at low enzyme loadings and the saturation point was confirmed at a weight ratio of 0.02. Ideal operating conditions were evaluated for pH and thermal stabilities. The optimum pH shifted from 4.0 to 5.0 after immobilization and the optimum temperature was 50 °C. Immobilized cellulase was demonstrated to have a marginal increase in stability over a wider range of temperatures as compared to free enzyme.

The reusability of the immobilized cellulase complex was assessed and was capable of withstanding six recycles while still retaining residual activity. The majority of activity loss (47.5%) occurred following the initial hydrolysis reaction and suffered a more gradual decline across the ensuing recycles. The activity of immobilized enzyme was determined to be 30.2% of the corresponding free enzyme activity.

Successful optimization of cellulase-bound nanoparticles achieved in this study could prove to have profound benefits for the ethanol industry. Future work would benefit from analyzing the superparamagnetic properties of the nanoparticles and determining the effects of binding on saturation magnetization. A more in-depth analysis of the nature of cellulase enzymes during hydrolytic reactions would also prove to be highly beneficial. One suggestion would be to determine individual sugar concentrations (i.e. glucose, cellobiose, and other polysaccharides) throughout the reactions in order to better understand the activities of each specific enzyme involved within the cellulase system. Future studies could also determine applications for recovering the immobilized enzymes after processing of cellulosic materials and offer a more economical approach for ethanol production.

References

[1] K.M. Ho, et al., Langmuir 24 (19) (2008) 11036–11042.
[2] W. Tischer, F. Wedekind, Immobilized Enzymes: Methods and Applications in Topics in Current Chemistry, 1999, pp. 95–126.
[3] U.T. Bornscheuer, Angewandte Chemie International Edition 42 (29) (2003) 3336–3337.
[4] B.R. Pieters, R.A. Williams, C. Webb, in: R.A. Williams (Ed.), Colloid and Surface Engineering: Applications in the Process Industries, Butterworth-Heinemann, Oxford, UK, 1992, pp. 248–286.
[5] A. Sharma, et al., IEEE Transactions on Magnetics 43 (6) (2007) 2418–2420.
[6] S.-H. Huang, M.-H. Liao, D.-H. Chen, Biotechnology Progress 19 (3) (2003) 1095–1100.
[7] S.V. Sonti, A. Bose, Journal of Colloid and Interface Science 170 (2) (1995) 575–585.
[8] Y. Zhang, N. Kohler, M. Zhang, BioMaterials 23 (2002) 1553–1561.
[9] A. Ito, et al., Journal of Bioscience and Bioengineering 100 (1) (2005) 1–11.
[10] V. Holzapfel, et al., Journal of Physics: Condensed Matter 18 (2006) S2581–S2594.
[11] A. Petri-Fink, et al., BioMaterials 26 (2005) 2685–2694.
[12] I. Hilger, R. Hergt, W.A. Kaiser, IEE Proceedings – Nanobiotechnology 152 (1) (2005) 33–39.
[13] J.B. Sundstrom, et al., Journal of Acquired Immune Deficiency Syndromes 35 (1) (2004) 9–21.
[14] M. Koneracka, et al., Journal of Magnetism and Magnetic Materials 201 (1–3) (1999) 427–430.
[15] X. Gao, et al., Chemical Communications (24) (2003) 2998–2999.
[16] M. Mikhaylova, et al., Chemistry of Materials 16 (12) (2004) 2344–2354.
[17] G.K. Kouassi, J. Irudayaraj, G. McCarty, BioMagnetic Research and Technology 3 (1) (2005).
[18] J. Hong, et al., Journal of Molecular Catalysis B: Enzymatic 45 (2007) 84–90.
[19] A.K. Johnson, et al., Journal of Nanoparticle Research (2007).
[20] H.P. Khng, et al., Biotechnology and Bioengineering 60 (4) (1998) 419–424.
[21] R. Stratulat, G. Calugaru, V. Badescu, Magnetic Carrier Particles for Selective Separation in Environmental and Industrial Processes, Anlele Stiintifice Ale Universitatii "AL.I.CUZA" IASI, 2000, pp. 45–50.
[22] M. Baalousha, et al., Environmental Toxicology and Chemistry 27 (9) (2008) 1875–1882.
[23] J. Zorjanovic, et al., International Symposium on Polymer Surface Modification: Relevance to Adhesion, Toronto, ON, Canada, 2007.
[24] P. Babinec, O. Jirsak, Optoelectronics and Advanced Materials, Rapid Communications 2 (8) (2008) 474–477.
[25] A. Garcia III, S. Oh, C.R. Engler, Biotechnology and Bioengineering 33 (1989) 321–326.
[26] D.-H. Chen, M.-H. Liao, Journal of Molecular Catalysis B: Enzymatic 16 (2002) 283–291.
[27] S. Oh, Enzymatic Hydrolysis of Cellulosic Biomass by Using Immobilized Cellulase, in Chemical Engineering, Texas Tech University, Dallas, TX, 1982.
[28] R.V. Mehta, et al., Biotechnology Techniques 11 (7) (1997) 493–496.
[29] M.M. Bradford, Analytical Biochemistry 72 (1976) 248–254.
[30] G.L. Miller, Analytical Chemistry 31 (3) (1959) 426–428.
[31] L. Brown, R. Torget, Enzymatic Saccharification of Lignocellulosic Biomass, Laboratory Analytical Procedure (LAP-009), NREL, 1996, pp. 1–8.
[32] T.K. Ghose, International Union of Pure and Applied Chemistry 59 (2) (1987) 257–268.
[33] L. Goldstein, Y. Levin, E. Katchalski, Biochemistry 3 (12) (1964) 1913–1919.
[34] L. Goldstein, E. Katchalski, Fresenius Zeitschrift Fur Analytische Chemie 243 (1968) 375–396.
[35] H. Weetall, Applied Biochemistry and Biotechnology 41 (1993) 157–188.
[36] T. Cha, A. Guo, X.-Y. Zhu, Proteomics 5 (2005) 416–419.

Jason Jordan graduated with a bachelor's degree in 2006 and master's degree in 2009, both in Biological & Agricultural Engineering from Louisiana State University. He is an active member of the American Society of Agricultural and Biological Engineers (ASABE) and is currently employed as an Agricultural Engineer with the USDA Grain Inspection, Packers and Stockyards Administration, Technical Services Division. He is part of the instrumental methods development team. His interests include bioprocessing, electrical/mechanical instrumentation, and bioenergy.

Challa S.S.R. Kumar is currently the Director of Nanofabrication & Nanomaterials at the Center for Advanced Microstructures and Devices (CAMD), Baton Rouge, USA. His research interests are in developing novel synthetic methods, including those based on micro-fluidic reactors, for multifunctional nanomaterials. He has also been involved in the development of innovative therapeutic & diagnostic tools based on nanotechnology. He has eight years of industrial R&D experience working for Imperial Chemical Industries and United Breweries. He is the founding Editor-in-Chief of the Journal of Biomedical Nanotechnology, published by American Scientific Publishers and Series editor for the two ten-volume book series, Nanotechnologies for the Life Sciences (NtLS) and Nanomaterials for the Life Sciences (NmLS) published by Wiley-VCH.

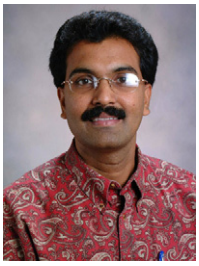

Chandra Theegala is currently working as an associated professor in the Biological and Agricultural Engineering (BAE) Department at Louisiana State University. Dr. Theegala holds a Ph.D. in Civil and Environmental Engineering from LSU. His doctoral research focused on mass production of weaker microalgal strains in open-unprotected environments. He is also the founder and group coordinator of the "Renewable Energy, Byproduct Utilization and Biosystems (REBUB)" research group in the BAE Department. In the energy arena, he is actively working on: biomass gasifiers, cost-effective microalgal cell harvesting & lipid extraction, hydrothermal liquefaction, cellulase recycling, solar drying, and geothermal heat pumps.